## Title
Case study of strong ground motion variation across cut slope



## Journal
Soil Dynamics and Earthquake Engineering, 25(7-10)

## Authors
Stewart, Jonathan P
Sholtis, Shawn E.

## Publication Date
2005

Peer reviewed

# CASE STUDY OF STRONG GROUND MOTION VARIATIONS ACROSS CUT SLOPE

by

**Jonathan P. Stewart**
Civil & Environmental Engineering Department
5731 Boelter Hall
University of California
Los Angeles, CA 90095-1593
jstewart@seas.ucla.edu
ph: 310 206 2990
fax: 310 206 2222

and

**Shawn E. Sholtis**
*City of Glendale, California*

To be published in

***Soil Dynamics and Earthquake Engineering***

Accepted for publication: September 12, 2004

Final version submitted: September 27, 2004

## ABSTRACT

We evaluate the influence of topography on motions recorded at the base and crest of an approximate 3H:1V, 20 m single-faced slope. The motions were recorded during the 1983 Coalinga earthquake mainshock and two aftershocks. Mainshock peak accelerations at the crest and base transverse to the slope face were 0.59g and 0.38g, respectively. The spectral amplification of crest motion occurred across $T \approx 0$ to 2 s. Differences between the crest/base motions are postulated to result principally from soil-structure interaction (base instrument is in a structure), variations in local ground response, and topography. Transfer functions quantifying soil-structure interaction (SSI) effects are evaluated and the base motion is modified at short periods to correct it to an equivalent free-field motion. The different levels of ground response at the crest and base are identified based on location-specific measurements of soil shear wave velocities. Differences between crest/base motions not accounted for by SSI or differential ground response are attributed to topographic effects. By these means, topographic spectral amplification (i.e., amplification relative to level ground conditions) is estimated to be about 1.2 at the crest and about 0.85-0.9 at the base across the period range $T \approx 0.4$–1.0 s.

## INTRODUCTION

Seismic body waves propagating towards the ground surface can be modified by near-surface geologic structure and surface topography. With respect to topographic effects, the issue of principal engineering interest is the modification of ground motion in areas near slopes relative to level ground conditions for a consistent subsurface geology. In this paper, we document a case history of topographic effects on strong ground motions recorded immediately above and below a cut slope during the $M_W = 6.4$ 1983 Coalinga earthquake mainshock and several aftershocks. The site under consideration is a water pumping plant, the location of which is shown in Figure 1. A cross section

through the site is shown in Figure 2, which shows a pumping plant structure at the base of the slope and a switchyard at the top of slope. The slope is approximately 20 m tall with an inclination of 3H:1V.

Mainshock motions were recorded by triaxial accelerographs mounted on the foundation of the pumping plant structure and in an instrument shelter in the switchyard. Peak horizontal accelerations (in both directions) were about 0.5g at the top-of-slope and about 0.3g at the base-of-slope. Differences in the recordings result principally from three effects; surface topography, different levels of local ground response, and soil-structure interaction effects associated with the pumping plant structure. In this paper we evaluate the differential ground response and soil-structure interaction effects so that the topographic effects on recordings from both locations can be estimated.

Previous studies have investigated the influence of topography on ground motion using both theoretical/numerical studies and observational field data. Theoretical/numerical studies of topographic effects have investigated amplification across isolated, two-dimensional, double-sided ridges that overlie a homogeneous halfspace [e.g., 1, 2], single-faced slopes [3, 4, 5], and canyons [e.g., 6, 7]. Most studies have focused on motions transverse to the slope, for which amplification levels are typically slightly greater than in the longitudinal direction [2]. Observational studies of topographic effects have generally either (1) documented concentrated damage patterns near the crests of ridges [8, 9, 10], (2) interpreted ground motion recordings of unexpectedly large-amplitude from single seismographs near ridge crests [11, 12], or (3) interpreted weak motion data from arrays across 2-D or 3-D surface geometries [e.g. 13, 14, 15, 16].

Only the third type of observational study is directly useful for validation of theoretical/numerical models of topographic effects. The available data applies principally to ridges,

with limited previous work for single-faced slopes. Moreover, most previous observational studies do not account for variations in ground response effects due to different geologic conditions at the base and crest of the slope. Accordingly, the levels of amplification attributed to topographic effects in previous observational studies have often far exceeded those expected from theoretical models [2]. As a result of this misinterpretation of field recordings, models for topographic effects remain, for most practical purposes, uncalibrated.

The present work is useful and original in that it provides a validation data set for topographic effects on single-faced slopes and it accounts for geologic amplification effects on the observed crest/base ground motion variations.

## SITE DESCRIPTION

As shown in Figure 2, the site consists of a pumping plant and adjacent canal that are located within a large excavation. Located immediately above the excavation southwest of the plant is an electric switchyard. The cut slope has an effective slope angle of 3H:1V and is approximately 15 to 21 m in height around the plant, approximately 21 m at the switchyard. The plant structure consists of a two-level building housing a series of water pumps and motors. The base of the structure is a concrete box 15 m by 61 m in plan view and 7 to 11 m in height. Located above this box is an 11m tall light steel frame providing cover for a pump service bay.

The site is located near the western edge of the San Joaquin Valley, California (Figure 1). The site is underlain by alluvial sediments that extend to depths of 300 to 600 m [17, 18]. Geotechnical properties of shallow soils were investigated using cone penetration testing (CPT) and a boring near the switchyard with a maximum depth of exploration of 122 m. Inferred soil conditions at the site based on subsurface exploration are summarized in Figure 3(a) for the switchyard location and Figure 3(b) for the plant location. The velocity data for the switchyard

location is derived from a nearby seismic CPT and suspension logging measurements in the boring. Data for the plant location is based on another seismic CPT and inference of suspension logging data from the switchyard for common elevations with appropriate corrections for differing overburden pressures [19]. The soils consist of interbedded, loose to medium dense, silty and clayey sands with occasional gravel layers. The plasticity index and fines content of the soil ranges from about 4-12 and 11-23%, respectively. The nonlinear properties of these soils were modeled using relationships for shear modulus reduction and damping for sands from [20].

## GROUND MOTION DATA

As shown in Figure 2, three strong motion accelerographs are located within the plant structure: at the base level 5.2 m below the plant grade, at plant grade, and on the roof of the steel frame for the service bay. An instrument is also located within the switchyard, 85 m southwest of the plant and 21 m above plant grade. The switchyard accelerograph is installed on a 1.3 m square concrete pad in a steel instrument shelter.

Recordings from the site are available from the May 2, 1983 $M_W$ = 6.4 Coalinga mainshock and aftershocks on May 9, 1983 ($M_W$ = 5.0) and July 22, 1983 ($M_W$ = 5.8) [21, 22]. Closest site-source distances for these events are 8.5, 14.6 and 17.4 km, respectively. Switchyard and plant base level recordings are available from each event. Peak accelerations, velocities and displacements at the two locations are listed in Table 1, and mainshock acceleration, velocity, and displacement waveforms are shown in Figure 4.

Plant motions are significantly smaller than switchyard motions, which can be attributed principally to the effects of soil-structure interaction, different levels of local ground response at the plant and switchyard, and topographic effects. As indicated in Table 1 and Figure 4, these differences are most pronounced in peak acceleration, but are non-negligible in velocity as well

displacement. As noted in [21], plant base- and grade-level motions are nearly identical, indicating nearly monolithic motion of the concrete box foundation. In the analyses that follow, emphasis is placed on motions transverse to the slope face, for which topographic amplification effects are expected to be maximized [2].

## SOIL-STRUCTURE INTERACTION EFFECTS

Some of the differences between the plant and switchyard motions are a result of kinematic soil-structure interaction (SSI) effects on the plant base-level motions. The kinematic constraint imposed upon a wave field by the embedded, stiff box foundation will tend to filter foundation motions relative to free-field motions. This filtering results principally from the embedment of the foundation and so-called "base slab averaging" effects associated with incoherent or inclined incident waves.

The kinematic SSI effects on foundation-level motions are quantified by a transfer function ($H_f$) relating the transverse motion at the base-level of the plant ($u_p$) to the "free-field" motion that would be expected at the plant location had the structure not been present ($u_{p,ff}$),

$$H_f(f) = \frac{u_p(f)}{u_{p,ff}(f)} \tag{1}$$

Motion $u_{p,ff}$ is referred to subsequently in the text as the modified plant (MP) motion. The transfer function amplitude was evaluated using available models for embedded foundations subject to vertically incident shear waves [23] and an empirical model for base slab averaging of shallow foundations [24]. The more significant of these effects for the present site is the embedment effect.

The resulting transfer function amplitude was used to scale the Fourier amplitude spectra of the plant base-level motions, which were then combined with the original phase spectra to calculate $u_{p,ff}$ through an inverse Fourier transform. Response spectra for the original and modified plant

motions transverse to the slope are presented in Figure 5 along with the spectra for the switchyard (top-of-slope) motion. As expected, the SSI modification enhances the high frequency components of $u_{p,ff}$ relative to $u_p$.

## RELATIVE GROUND RESPONSE EFFECTS

Ground response effects are different at the plant and switchyard locations as a result of different shear wave velocities of the underlying soils (Figure 3). Accordingly, analyses were performed to evaluate the relative levels of ground response at the plant and switchyard.

Those analyses involved the calculation for both the plant and switchyard locations of transfer functions associated with 1D vertical propagation of shear waves through the soil. It is necessary to use 1D models (even though the site geometry is more nearly 2D) because the intent of these calculations is to identify the relative ground response effects so that the remaining difference (due to 2D topographic effects) can be estimated. Each of these transfer functions represent variations in ground motion amplitude between the surface and an elevation within the soil profile for which the seismic velocities at the plant and switchyard locations are comparable (this depth was taken as 122 m below the switchyard, but the outcome of the analyses is insensitive to the selected depth). The calculations were carried out with equivalent-linear ground response analysis procedures [25] using location-specific velocity profiles and de-convolved motions for the 122 m depth derived from $u_s$ and $u_{p,ff}$. The motions calculated at the ground surface from these analyses are denoted $u_{s,1D}$ for the switchyard (SY) and $u_{p,ff,1D}$ for the modified plant (MP). Additional details on these analyses are presented in [26].

The results are presented in Figure 6 as the ratio of the response spectra (RRS) for motions $u_{s,1D}/u_{p,ff,1D}$ from the mainshock and an aftershock. This RRS represents the relative effect of the different velocity profiles on the expected spectral accelerations based on 1D analysis. There is

small variability in the results for a given earthquake because of slightly different 1D ground responses associated with the different de-convolved motions. The curves in Figure 6 are averages across the different motions.

Results for the two events with strong and relatively weak motions are similar. Relative amplification factors are as large as 1.4 for periods between about 0.4 and 1.0 s, which is associated with relatively soft soils near the surface at the switchyard. The relative ground response effect is not significant outside of that period range.

The results in Figure 6 and subsequent figures are presented across the period range $T$ = 0.2-3 s. Longer periods are not plotted because the data are not reliable as a result of high-pass filtering used during data processing. Shorter periods are not plotted because of non-physical fluctuations in the RRS functions, which likely result from numerical errors in the de-convolution analyses. Such errors at high frequencies are commonly associated with the use of de-convolved motions [27, 28]. Since independent validation of the soil-structure interaction and relative ground response effects is not possible with the available strong motion data, we can not rigorously confirm that the results are accurate across the central period range of $T$ = 0.2-3 s. However, since the engineering models for those analyses have been previously validated against case histories, our expectation is that the results in Figure 6 and subsequent figures provide reasonable first-order estimates of the effects considered.

## EVALUATION OF TOPOGRAPHIC AMPLIFICATION EFFECT

Figure 7 illustrates the SY/MP RRS as calculated directly from the motions $u_s$ and $u_{p,ff}$ (thick line), along with the relative ground response RRS from Figure 6, i.e., $u_{s,1D}/u_{p,ff,1D}$ (thin line). The thick-line RRS represents the differences between the SY and MP motions associated with both geologic and topographic amplification. Results are presented for the mainshock, but the aftershock data

shows similar trends [26]. From Figure 7, the geologic amplification effect (i.e., the amplification illustrated with the 1D analysis results) is seen to contribute significantly to the total amplification for periods up to about 3 s.

The offset between the thick and thin lines in Figure 7 represents the estimated topographic effect on the SW/MP ground motion variations. It should be noted that these topographic effects include amplification at SY and de-amplification at MP. For all three events investigated, the topographic amplification is most pronounced across the period range $T$ = 0.4 to 1.0 s, for which the maximum amplification is approximately 1.4. This period range corresponds to wavelengths of about 80 – 200 m (approximately 4-9 × slope height). This bandwidth of topographic amplification is fairly consistent with the findings of [3] that topographic amplification of single-faced slopes is most pronounced at wavelength = 5 × slope height

The issue of principal engineering interest is the expected modification of ground motion in areas near slopes relative to level ground conditions for a consistent subsurface geology. We provide this representation of topographic effects on the MP and SY motions by evaluating for each location RRS of the total motion (which includes geologic and topographic effects) to calculated motions from the 1D analysis (which lacks the topographic effect). Results for all three events are summarized in Figure 8(a) for SY and Figure 8(b) for MP. The maximum topographic amplification at SY is about 20%, and occurs across the period range $T \approx$ 0.4 - 1.0 s. The largest de-amplification of MP is about 10-15%, which occurs across the same period range.

Also shown in Figure 8(a) is the transfer function amplitude from [4] for a 30 degree slope with vertically incident waves (dashed line). The amplification levels of the model and data are comparable. However, the data indicates more narrowly banded amplification than predicted by the model.

Ref. [26] presents the results from Figures 7-8 in the form of transfer functions as well as response spectral ratios. When measured using transfer functions, the amplitude of SY amplification and MP de-amplification was more variable, but generally similar in magnitude to the response spectral ratios shown above. The period range across which SY amplification and MP de-amplification were observed was similar for the transfer function and response spectral ratio approaches.

## SUMMARY AND CONCLUSIONS

The objective of this study was to evaluate topographic effects on strong ground motions recorded above and below a single-faced slope during the 1983 Coalinga earthquake mainshock and two aftershocks. Recorded motions at the crest of the slope were significantly larger than those at the base, which is attributed to soil-structure interaction effects (on base motions, which were recorded in a structure), as well as differential ground response and topographic amplification effects. To isolate the topographic effects on the ground motion at the crest and base of the slope, the soil-structure interaction and differential ground response effects were removed using established engineering models.

Soil-structure interaction was found to affect the base motion principally at small periods ($T < 0.35$ s). Geologic amplification significantly contributed to the amplification observed at the crest relative to the base for periods up to about 3 s. The remaining crest/base amplification is attributed to topographic effects. Topographic effects are most pronounced for $T \approx 0.4$-1.0 s (wavelengths ≈ 4-9 slope heights), which is reasonably consistent with the recommendations of [3]. Across the period range of $T \approx 0.4$-1.0 s, approximately half of the observed amplification is due to geologic effects in each of the three events.

Using spectral ratios of recorded (crest) and recorded/SSI-corrected (base) motions to 1D

calculated motions, the maximum topographic amplification at the slope crest is found to be approximately 1.2 (i.e., 20% greater than the anticipated motion at a level site), and the maximum topographic de-amplification at the slope base is on the order of 0.85-0.9 (i.e., 10-15% less than the anticipated motion at a level site). This magnitude of crest spectral amplification (about 1.2) is consistent with amplification levels predicted by the models presented in Ref. [4] for vertically propagating waves.

**ACKNOWLEDGEMENTS**

Support for this work was provided by the U.S. Geological Survey, National Earthquake Hazards Reduction Program, Award No. 1434-HG-98-GR-00038. This support is gratefully acknowledged. The views and conclusions contained in this document are those of the authors and should not be interpreted as necessarily representing the official policies, either expressed or implied, of the U.S. Government.

**REFERENCES**

[1] Bard, P-Y. (1995). Effects of surface geology on ground motion: recent results and remaining issues, in *10th European Conference on Earthquake Engineering*, Duma (ed.), Rotterdam, 305-323.

[2] Geli, L., P-Y. Bard, and B. Jullien (1988). The effect of topography on earthquake ground motion: a review and new results, *Bull. Seism. Soc. Am.*, **78** (1), 42-63.

[3] Ashford, S.A. and N. Sitar (1997). Analysis of topographic amplification of inclined shear waves in a steep coastal bluff, *Bull. Seism. Soc. Am.*, **87** (3), 692-700.

[4] Ashford, S.A., N. Sitar, J. Lysmer, and N. Deng (1997). Topographic effects on the seismic response of steep slopes, *Bull. Seism. Soc. Am.*, **87** (3), 701-709.

[5] Sitar, N. and G.W. Clough (1983). Seismic response of steep slopes in cemented soils, *J. Geotech. Engrg.* **109** (2), February.

[6] Trifunac, M.D. (1973). Scattering of SH waves by a semi cylindrical canyon, *Earthquake Engrg. Struct. Dyn.*, **1** (3), 267-281.

[7] Wong, H.L. and M.D. Trifunac (1974). Scatting of plane SH waves by a semi-elliptical canyon, *Earthquake Engineering Struct. Dyn.*, **3** (2), 157-169.

[8] Celebi, M. (1987). Topographical and geological amplifications determined from strong-motion and aftershock records of the 3 March 1985 Chile earthquake, *Bull. Seism. Soc. Am.*, **77** (4), p 1147-1167.

[9] Kawase, H. and K. Aki (1990). Topography effect at the critical SV-wave incidence: Possible explanation of damage pattern by the Whittier Narrows, California, earthquake of 1 October 1987, *Bull. Seism. Soc. Am.*, **80** (1), 1-22.

[10] Sitar, N., S.A. Ashford, J.P. Stewart, L. Nova-Roessig (1997). Seismic response of steep natural slopes, structural fills, and reinforced soil slopes and walls, in *Proc. 14$^{th}$ Int. Conf. on Soil Mechanics and Foundation Engrg.*, Hamburg Germany.

[11] Spudich, P., M Hellweg, and W.H.K. Lee (1996). Directional topographic site response at Tarzana observed in aftershocks of the 1994 Northridge, California, Earthquake: Implications for mainshock motions, *Bull. Seism. Soc. Am.*, **86** (1B), S139-S208.

[12] Trifunac, M.D. and D.E. Hudson (1971). Analysis of the Pacoima Dam accelerograms – San Fernando earthquake of 1971, *Bull. Seism. Soc. Am.*, **61** (5), 1393-1411.

[13] Davis, L.L. and L.R. West (1973). Observed effects of topography on ground motion, *Bull. Seism. Soc. Am.*, **63** (1), 283-298.

[14] Hartzell, S.H., D.L. Carver, K.W. King (1994). Initial investigation of site and topographic effects at Robinwood Ridge, California, *Bull. Seism. Soc. Am.*, **84** (5), 1336-1349.

[15] Pedersen, H.A., B. Le Brun, D. Hatzfeld, M. Campillo, and P.-Y. Bard (1994). Ground motion amplification across ridges, *Bull. Seism. Soc. Am.*, **84** (6), 1786-1800.

[16] Tucker, B.E., J.L. King, D. Hatzfeld, and I.L. Nersesov (1984). Observations of hard-rock site effects, *Bull. Seism. Soc. Am.*, **74** (1), 121-136.

[17] Bureau of Reclamation (1974). *Technical record of design and construction, Central Valley Project, West San Joaquin Division, San Luis unit, California, volume 1, history, general description and geology*, U.S. Dept. of the Interior, Denver, CO.

[18] Davis, G.H. and J.F. Poland (1957). Ground-water conditions in the Mendota-Huron Area, Fresno and Kings Counties, CA, U.S. Geological Survey, Water Supply Paper 1360-G.

[19] Seed, H.B. and I.M. Idriss (1970). Soil moduli and damping factors for dynamic response analysis, Earthquake Engineering Research Center, Univ. of California, Berkeley, Rpt. EERC 70-10.

[20] EPRI (1993). *Guidelines for Determining Design Basis Ground Motions. Volume 1: Methods and Guidelines for Estimating Earthquake Ground Motion in Eastern North America*. Report No. EPRI TR-102293, Palo Alto, CA.

[21] Maley, R., G. Brady, E. Etheredge, D. Johnson, P. Mork, and J. Switzer (1984). Analog strong motion data and processed main-event recordings obtained by U.S. Geological Survey near Coalinga, CA, in *Coalinga, California, Earthquake of May 2, 1983, Reconnaissance Report*, EERI, Oakland, CA, 75-88.

[22] Seekins, L.C., G. Brady, C. Carpenter and N. Brown (1992). Digitized Strong-Motion Accelerograms of North and Central American Earthquakes 1933-1986, U.S. Geological Survey Digital Data Series DDS-7.

[23] Elsabee, F. and J.P. Morray (1977). Dynamic response of arbitrarily shaped foundations, Dept. of Civil Engrg., MIT, Cambridge, Mass., *Rpt. No. R77-33*.

[24] Kim, S. and J.P. Stewart (2003). Kinematic soil-structure interaction from strong motion recordings, *J. Geotech.. & Geoenv. Engrg.*, ASCE, **129** (4), 323-335.

[25] Idriss, I.M. and J.I. Sun (1991). SHAKE91: A computer program for equivalent liner seismic response analyses of horizontally layered soil deposits, Dept. of Civil Engineering, U.C. Davis.

[26] Sholtis, S.E. and J.P. Stewart (1999). Topographic amplification across cut slope in sand, Department of Civil & Environmental Engineering, University of California, Los Angeles.

[27] Idriss, I.M., and M.R. Akky (1979). Primary variables influencing generation of earthquake ground motions by a deconvolution process, in *Proc. 5$^{th}$ SMIRT*, Vol. K(a).

[28] Silva, W.J. (1986). Soil response to earthquake ground motion, Electrical Power Research Institute, Palo Alto, CA, Rpt. No. RP2556-07.

**Table 1: Summary of strong motion recordings at plant base-level and switchyard**

| | | Plant Base-Level | | | Switchyard | | |
|---|---|---|---|---|---|---|---|
| | | acc (g) | vel (cm/s) | dis (cm) | acc (g) | vel (cm/s) | dis (cm) |
| MS | v | 0.21 | 12.2 | 2.5 | 0.35 | 16.1 | 2.3 |
| | tr (045) | 0.38 | 32.4 | 6.4 | 0.59 | 60.2 | 8.8 |
| | ln (135) | 0.29 | 19.1 | 2.6 | 0.55 | 36.3 | 4.0 |
| AS1 | v | 0.04 | 1.4 | 0.2 | 0.10 | 2.6 | 0.3 |
| | tr (045) | 0.05 | 5.8 | 0.7 | 0.10 | 7.7 | 1.0 |
| | ln (135) | 0.13 | 6.5 | 0.5 | 0.21 | 9.9 | 0.7 |
| AS2 | v | 0.13 | 5.9 | 2.5 | 0.32 | 12.8 | 0.9 |
| | tr (045) | 0.41 | 18.9 | 5.7 | 0.60 | 34.8 | 8.1 |
| | ln (135) | 0.23 | 21.6 | 6.2 | 0.33 | 12.0 | 2.3 |

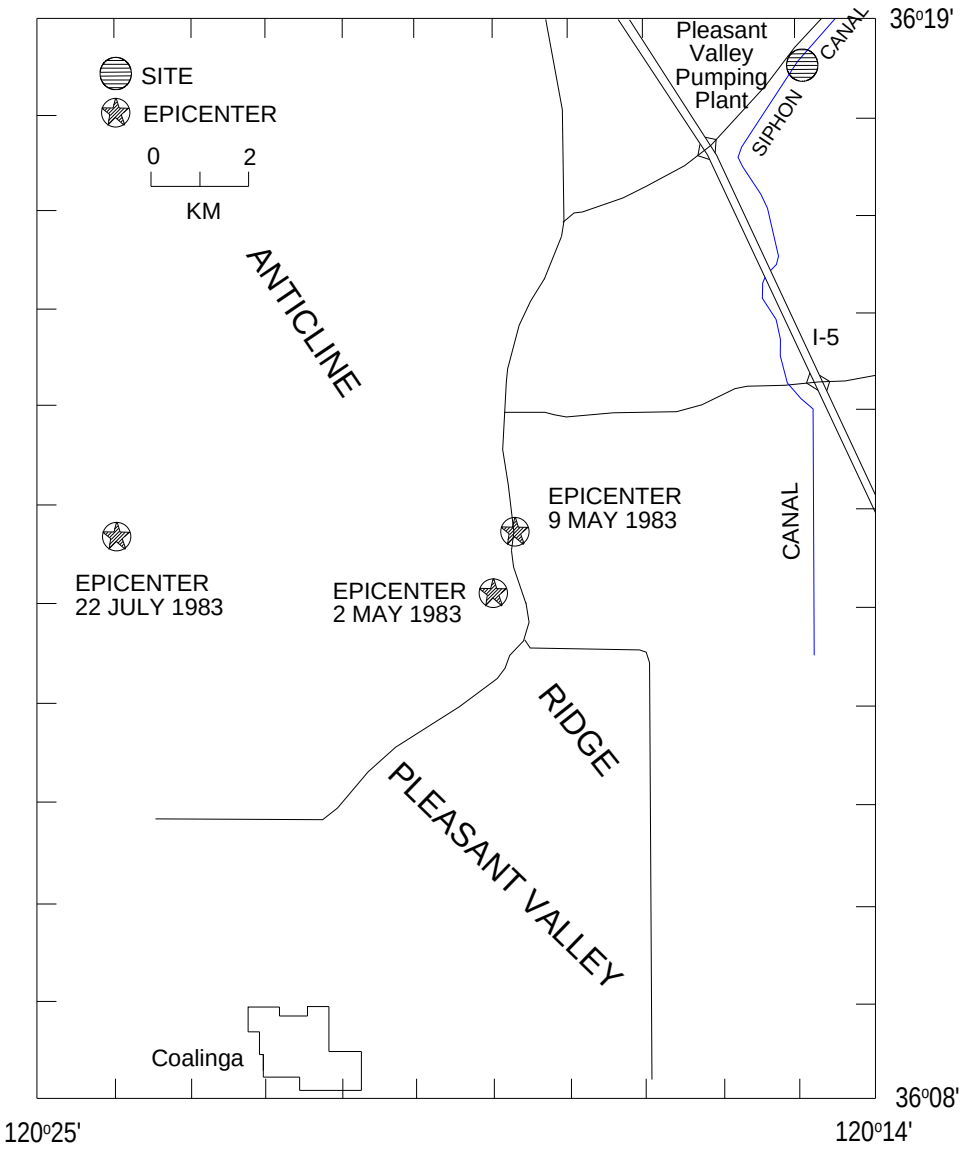


**Fig. 1: Site location and event epicenter locations**

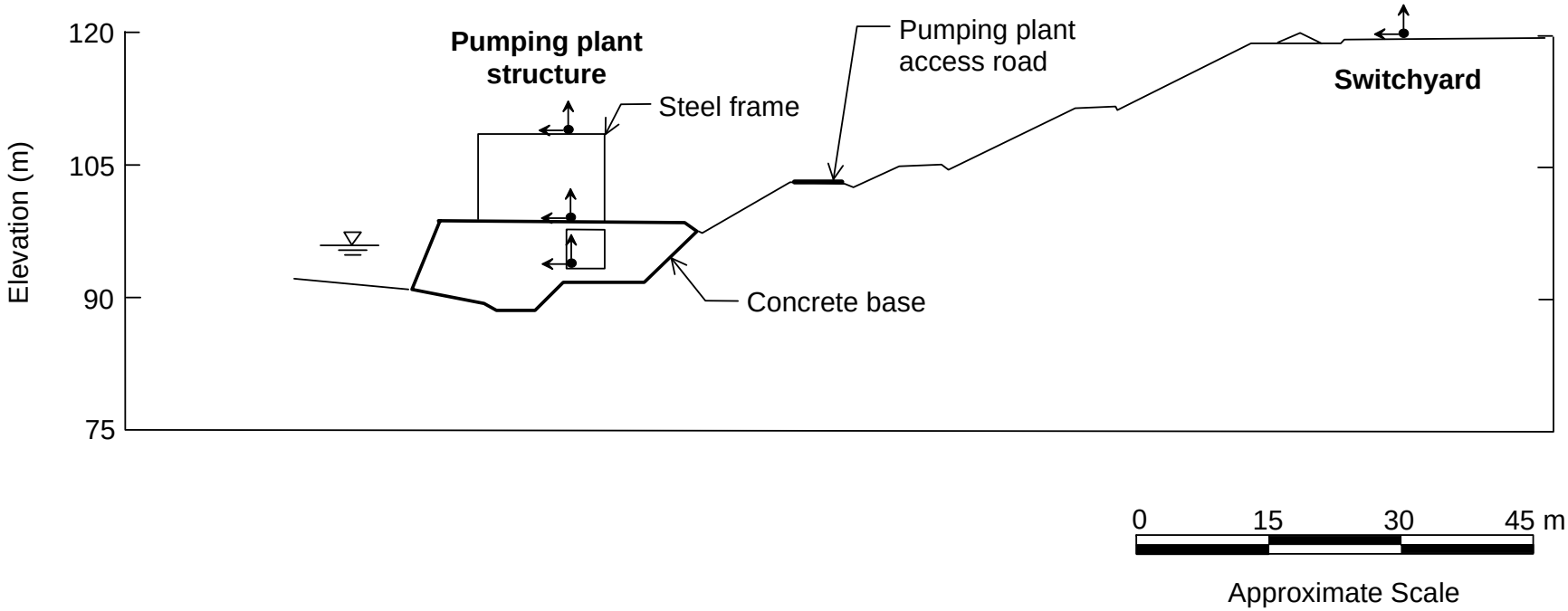


**Fig. 2: Cross section through pumping plant site showing locations of strong motion accelerographs**

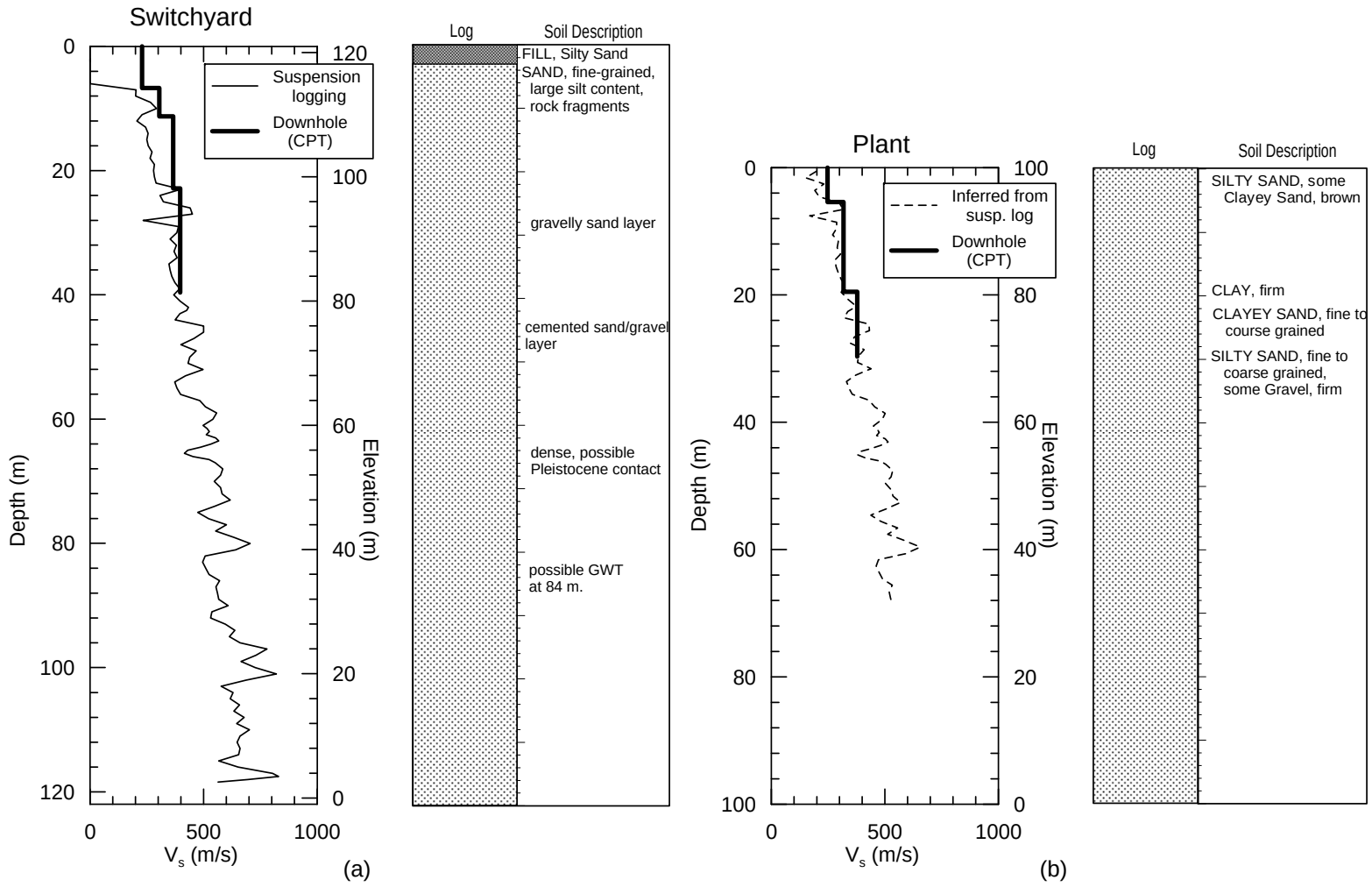


**Fig. 3: Soil and shear wave velocity profiles at switchyard and plant**

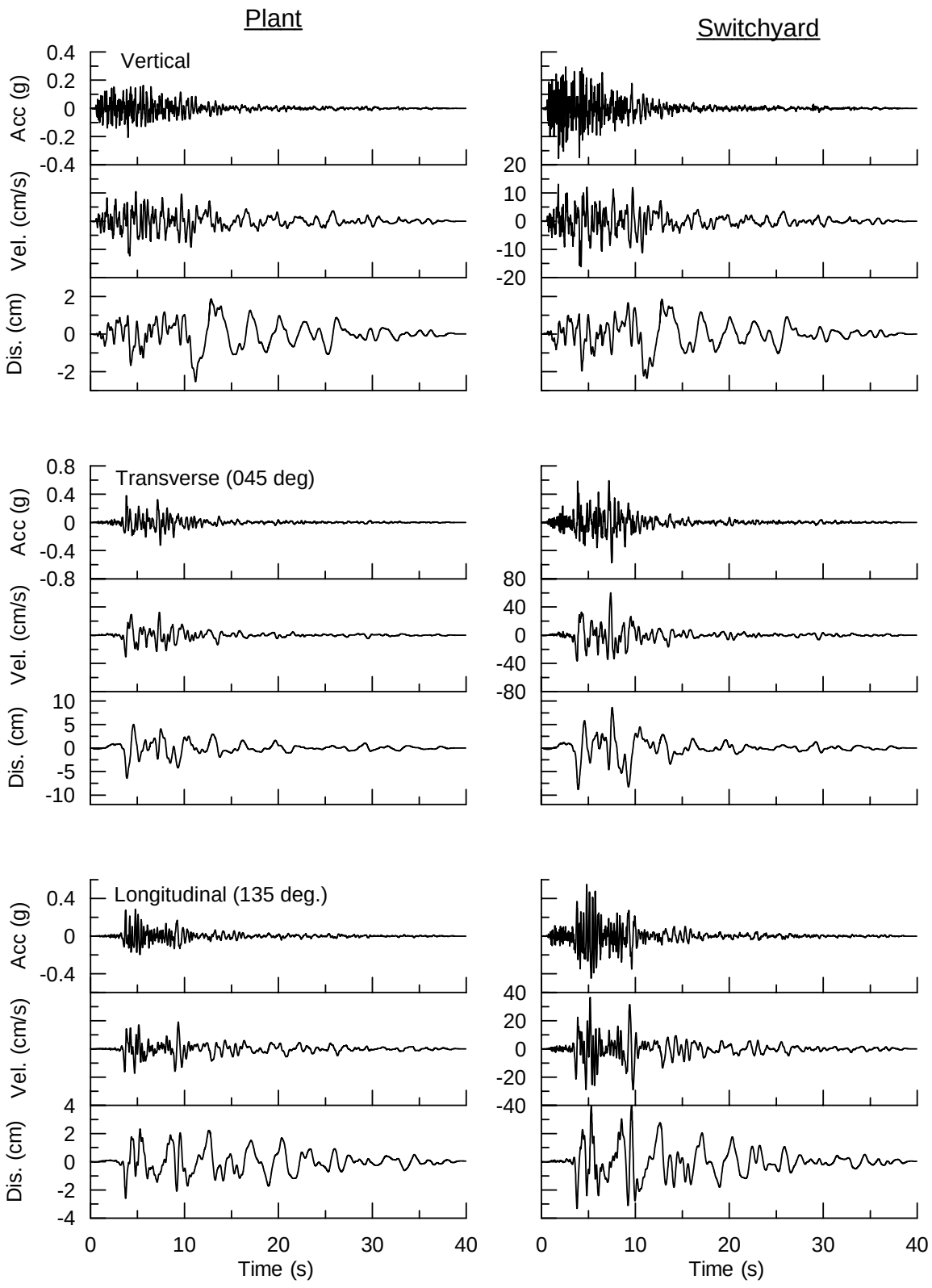


**Fig. 4: Acceleration, velocity, and displacement waveforms from 1983 Coalinga earthquake mainshock and aftershock recorded in pumping plant and switchyard**

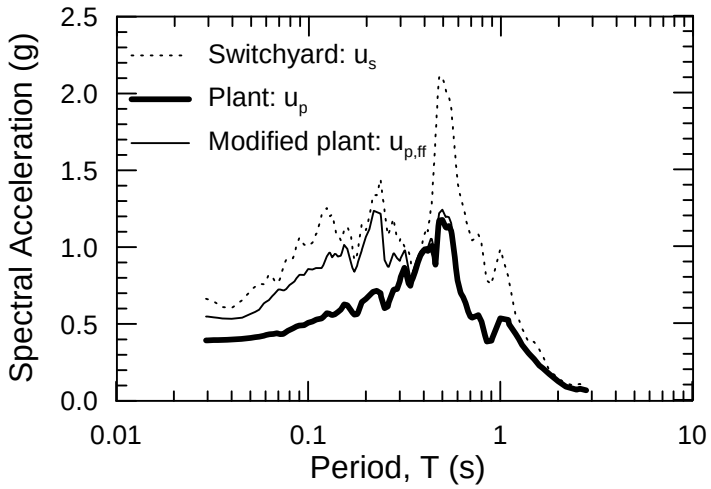


**Fig. 5: 5%-damped response spectra for plant and switchyard mainshock motions transverse to the slope face, along with modified plant motion for SSI**

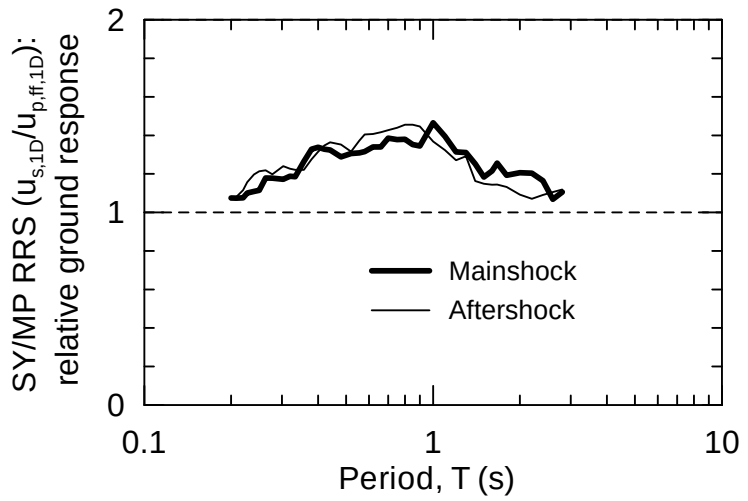


**Fig. 6: Average 5%-damped ratio of response spectra (RRS) for plant and switchyard locations associated with relative ground response**

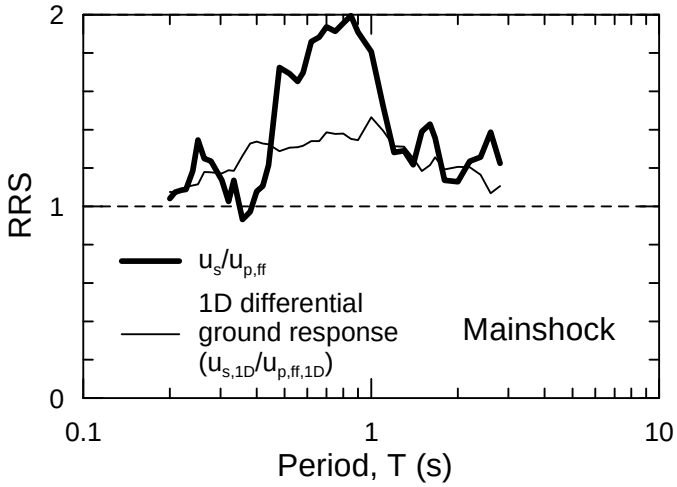


**Fig. 7: Ratio of response spectra (5% damping) for SW/MP motions based on recordings (representing topographic and differential ground response amplification effects) and 1D analysis (representing estimated contribution from differential ground response)**

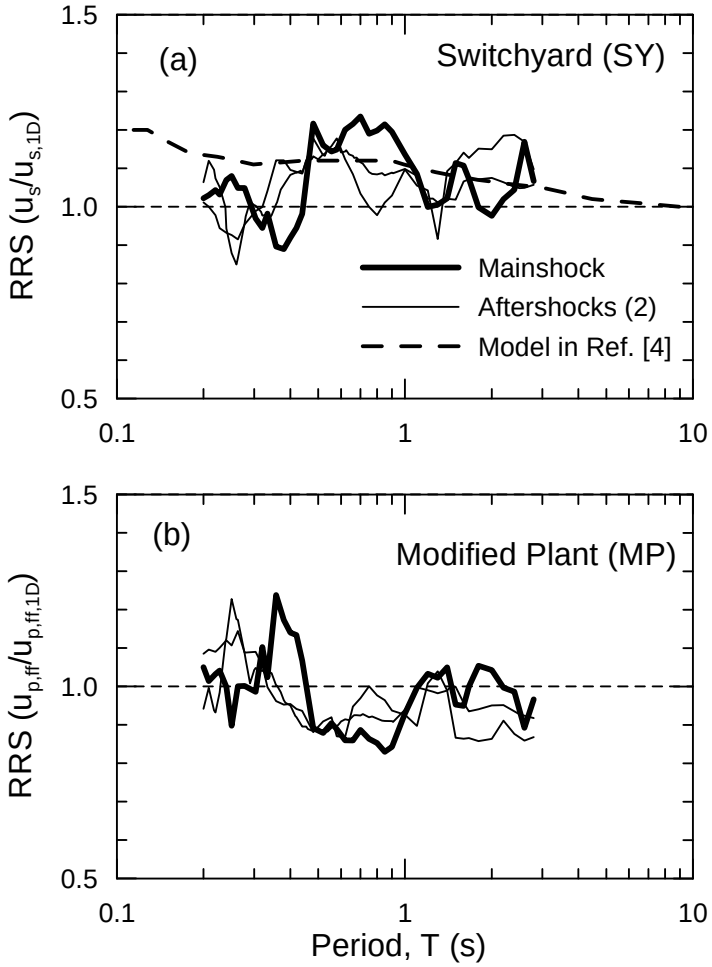


**Fig. 8: Median RRS of SY and MP motions (transverse to slope) to 1D calculated motions for mainshock and two aftershocks**